Positive Feedback Between PU.1 and the Cell Cycle Controls Myeloid Differentiation

Hao Yuan Kueh,[1]* Ameya Champhekar,[1] Stephen L. Nutt,[2] Michael B. Elowitz,[1,3] Ellen V. Rothenberg[1]*

Regulatory gene circuits with positive-feedback loops control stem cell differentiation, but several mechanisms can contribute to positive feedback. Here, we dissect feedback mechanisms through which the transcription factor PU.1 controls lymphoid and myeloid differentiation. Quantitative live-cell imaging revealed that developing B cells decrease PU.1 levels by reducing PU.1 transcription, whereas developing macrophages increase PU.1 levels by lengthening their cell cycles, which causes stable PU.1 accumulation. Exogenous PU.1 expression in progenitors increases endogenous PU.1 levels by inducing cell cycle lengthening, implying positive feedback between a regulatory factor and the cell cycle. Mathematical modeling showed that this cell cycle–coupled feedback architecture effectively stabilizes a slow-dividing differentiated state. These results show that cell cycle duration functions as an integral part of a positive autoregulatory circuit to control cell fate.

The transcription factor PU.1 is a central component of the regulatory gene network controlling lymphoid and myeloid development from hematopoietic progenitors (*1*–*4*). PU.1 is expressed at intermediate levels in progenitors, and its subsequent levels become a determinant of lymphoid and myeloid fate choices, with down-regulation of PU.1 required for B and T cell development and higher PU.1 levels favoring the development of macrophages or myeloid dendritic cells (*5*–*8*).

Differential regulation of PU.1 during lymphoid and myeloid development involves transcriptional positive feedback of PU.1 (*9*). PU.1 positively regulates its own transcription in myeloid cells and stem cells, but not in lymphoid cells (*10*–*13*), and forms additional positive-feedback loops through mutual inhibition with other hematopoietic regulators (*7*, *14*). Positive feedback can, in principle, generate multiple stable states with different levels of regulatory factors, possibly accounting for the observed differences in PU.1 levels. However, it is unclear how PU.1 is regulated during myeloid or lymphoid development, what feedback mechanisms are involved, and why particular feedback architectures may have been selected.

PU.1 promotes growth in several progenitor types (*1*, *15*), but also coordinates cell cycle arrest with differentiation in myeloid progenitors. Reduced PU.1 activity causes acute myeloid leukemia, where progenitors fail to initiate differentiation growth arrest (*16*–*19*); conversely, reexpression of PU.1 restores growth arrest (*17*, *20*, *21*). However, it is unclear whether PU.1's effect on the cell cycle influences its ability to regulate its own levels and control differentiation.

In this work, we analyzed PU.1 and cell cycle regulation in individual cells during early macrophage and B cell development (Fig. 1A). We isolated fetal liver progenitors (FLPs, Lin$^-$cKit$^+$CD27$^+$) from mice containing a bicistronic PU.1–green fluorescent protein (GFP) knock-in reporter (*2*), cultured them with cytokines supporting B cell and macrophage differentiation, and analyzed PU.1-GFP levels over time by time-lapse imaging or flow cytometry (Fig. 1 and figs. S1 and S2) (*22*). PU.1-GFP levels varied linearly with nuclear PU.1 protein levels in this culture system (fig. S3). We found that progenitors initially expressed PU.1-GFP at uniform levels but subsequently up- or down-regulated PU.1-GFP over time (Fig. 1, B to D, and fig. S4). Cells up-regulating PU.1-GFP expressed the macrophage markers CD11b and F4/80, but not the granulocyte marker Gr1, and were also large and adherent, reflecting differentiation into macrophages [Fig. 1, B and C (top right), and fig. S4]. In contrast, cells down-regulating PU.1-GFP expressed the B cell marker CD19 and were also small and round, reflecting differentiation into B cells [Fig. 1, B and C (bottom right), and figs. S2 and S4). Developing granulocytes and persisting progenitor-like cells maintained PU.1-GFP levels similar to those of starting progenitors (Fig. 1B and fig. S4). Both macrophages and B cells preferentially developed from Fcγ receptor II/III (FcγR2/3)^{low} FLPs, whereas FcγR2/3$^+$ FLPs mostly differentiated into granulocytes (fig. S5 and see below). These results validate the use of our system for analyzing PU.1 regulation during B cell or macrophage differentiation.

Changes in PU.1 levels during B cell or macrophage differentiation may result from changes in either the rate of PU.1 synthesis or the rate of PU.1 removal (Fig. 1E), which would occur predominantly through dilution due to cell division (*23*, *24*), as PU.1's protein half-life is substantially longer than the progenitor cell cycle length (fig. S6). To determine how PU.1 levels were regulated, we measured PU.1 synthesis rates and cell cycle lengths for individual cells within defined progenitor, macrophage (Mac), and B cell populations (Fig. 1D and fig. S7). PU.1 synthesis rates could be measured by the slopes of stable PU.1-GFP increase over time [($\Delta p/\Delta t$ for an observed cell cycle; p, GFP or PU.1 protein; t, time), Fig. 1E and fig. S7; fig. S8 shows GFP stability], independent of average PU.1-GFP levels. Although cell movement precluded comprehensive multigenerational tracking (fig. S9), we analyzed time-lapse movies that allowed accurate measurements of average cell cycle lengths and PU.1 synthesis rates for different cell populations. Progenitors comprised two subpopulations with higher and lower rates of PU.1 synthesis (Fig. 1, F and G). Switches between states with high and low PU.1 synthesis rates were infrequent across cell division (Fig. 1G), suggesting that these states are maintained stably in most cells. Macrophages had more PU.1-GFP and PU.1 protein than any of the progenitors (Fig. 1H and fig. S3), as expected. Surprisingly, however, their PU.1 synthesis rates were not higher than that of the progenitor subpopulation with high PU.1 synthesis rates (Fig. 1, F to H, and fig. S9). Instead, macrophages had significantly longer cell cycle lengths (Fig. 1, F to H, and fig. S9) and descended from ancestors with shorter cell cycle lengths but similar PU.1 synthesis rates (Mac early, Fig. 1, F to H). Thus, developing macrophages increase their PU.1 levels by lengthening their cell cycles, which allows PU.1 to accumulate to higher levels. In contrast, emerging B cells had significantly lower PU.1 synthesis rates than progenitors but similar cell cycle lengths (Fig. 1, F to H, and fig. S9). Therefore, unlike macrophages, B cells decrease PU.1 levels by reducing PU.1 transcription.

Increased PU.1 levels caused by cell cycle lengthening may be functionally important for macrophage differentiation or may simply reflect a consequence of differentiation growth arrest (Fig. 2A). To distinguish between these two possibilities, we tested whether artificial cell cycle lengthening promotes myeloid differentiation in a PU.1-dependent manner. We induced cell cycle lengthening in FLPs by two different methods: either by retroviral transduction of cyclin-dependent kinase (CDK)–inhibitors p21^{Cip1} (Cdkn1a) or p27^{Kip1} (Cdkn1b) (Fig. 2B and fig. S10) or by treatment with PD0332991, a CDK4/6 inhibitor (*25*) (Fig. 2, C and D). Induced cell cycle lengthening in progenitors increased PU.1-GFP and PU.1 protein levels and the percentage of myeloid cells, with these increases being most dramatic in the slowest-dividing cells (Fig. 2, B and C). This differentiation depended on PU.1 activity, because in cells transduced with a competitive inhibitor of PU.1 (PU.1-ets) (fig. S11), PD0332991 treatment still increased PU.1-GFP, but no longer increased the fraction of CD11b-expressing cells as in empty vector (EV)–transduced cells (Fig. 2, C and D). These results suggest that PU.1 accumulation as a result of cell cycle lengthening is functionally important for macrophage differentiation.

[1]Division of Biology, California Institute of Technology, Pasadena, CA, USA. [2]The Walter and Eliza Hall Institute of Medical Research, Parkville, Victoria, Australia. [3]Howard Hughes Medical Institute and Department of Bioengineering, California Institute of Technology, Pasadena, CA, USA.

*Corresponding author. E-mail: kueh@caltech.edu (H.Y.K.); evroth@its.caltech.edu (E.V.R.)

To examine how positive transcriptional feedback regulates PU.1's own expression (*10*–*13*), we tested how PU.1 and dominant negative PU.1 transduction affected transcription of the PU.1-GFP reporter. Forced expression of PU.1-ets in FLPs reduced PU.1-GFP levels (fig. S12), implying that a threshold level of PU.1 activity is important for maximal PU.1 expression. Conversely, flow cytometry and imaging showed that exogenous PU.1 up-regulated PU.1-GFP and CD11b while inhibiting PU.1-GFP down-regulation and CD19 up-regulation (Fig. 3, A and B, and fig. S13). However, imaging analysis (Fig. 1E) showed that exogenous PU.1 expression did not increase endogenous PU.1 synthesis rates; instead, it induced cell cycle lengthening in a subpopulation of progenitors, which led to the increase in PU.1-GFP levels (Fig. 3, C and D, and fig. S14). This cell cycle lengthening occurred preferentially in FcγR2/3^{low} FLPs (fig. S5C), which accounted for most of the macrophage potential in the FLP population. Thus, high PU.1 levels promote cell cycle lengthening in cells capable of generating macrophages, which, in turn, allows high PU.1 levels to be stably maintained. Taken together, our results provide evidence for a regulatory circuit architecture involving positive feedback on a transcription factor through the cell cycle.

Insight into cell cycle lengthening mechanisms emerged from analysis of regulatory gene expression in PU.1-transduced progenitors (Fig. 3E). Consistent with PU.1 autoregulation through cell cycle lengthening rather than transcriptional acceleration, PU.1 transduction did not affect endogenous PU.1 mRNA levels, but it reduced the levels of cell cycle promoting factors cyclin D2 (Ccnd2) and Cdc25a. Consistent with other studies (*26*–*28*), exogenous PU.1 also reduced the levels of Myb and Myc, growth-promoting proto-oncogenes that are down-regulated during normal differentiation. Exogenous PU.1 also reduced levels of p21 and Gfi1, which can mediate quiescence, although these are up-regulated by PU.1 in stem cells (*13*). Thus, the mechanisms underlying PU.1-mediated cell cycle arrest during macrophage differentiation appear distinct from those operating in stem cell quiescence.

How can positive feedback between PU.1 and the cell cycle stabilize a slow-dividing macrophage state with high PU.1 levels? To address this issue, we constructed a stochastic single-cell dynamical model, where PU.1 inhibits the G_1-to-S cell cycle transition above a threshold concentration (Fig. 4A, top). This model exhibits bistability, supporting both a fast-dividing, low-PU.1 state and a slow-dividing, high-PU.1 state (Fig. 4A and figs. S15 and S16). In our simple model, G_1 checkpoint release depends solely on PU.1 levels; during macrophage development, other regulatory factors also promote checkpoint release and, thus, may regulate feedback engagement. Once the high PU.1 state is established, it is relatively stable compared with the corresponding state of a hypothetical pure transcriptional feedback system with similar parameters, which exhibits more frequent spontaneous switches between states due to

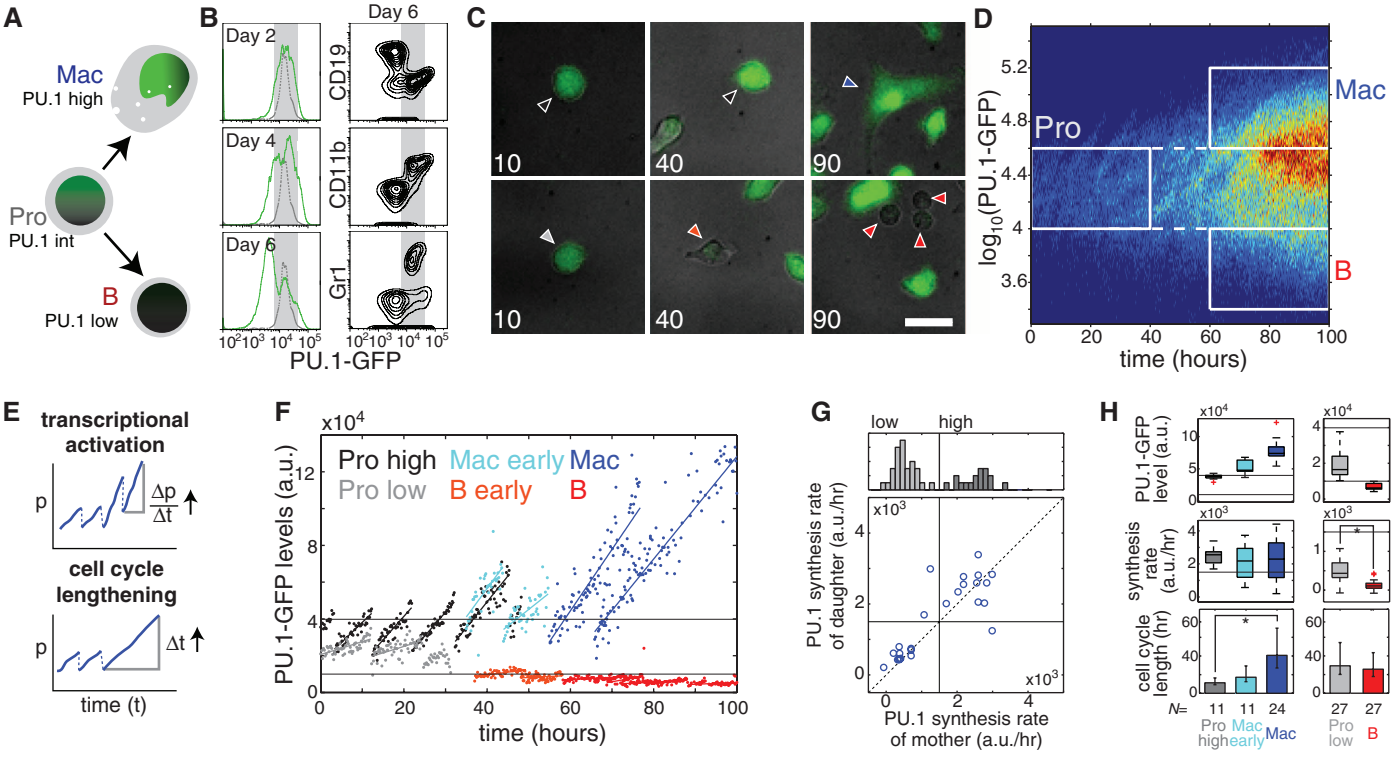

Fig. 1. Cell cycle lengthening drives PU.1 up-regulation during macrophage development. FLPs (Lin-cKit$^+$CD27$^+$) from embryonic day 13.5 PU.1-GFP mice were cultured with B cell– and macrophage-supporting cytokines [stem cell factor (SCF), interleukin-3 (IL-3), IL-7, Flt3L, macrophage colony-stimulating factor] and analyzed with time-lapse imaging or flow cytometry. (**A**) Schematic showing myeloid and lymphoid development from hematopoietic progenitor cells. Mac, macrophage; Pro, progenitor, B, B cell. (**B**) Histograms (left) show PU.1-GFP levels measured after the indicated number of days in culture. Dotted lines give initial PU.1-GFP levels. Flow cytometry plots (right) show CD19, CD11b, and Gr-1 levels against PU.1-GFP after 6 days. (**C**) Merged differential interference contrast (gray) and PU.1-GFP fluorescence (green) images of cultured FLPs, taken after the indicated number of hours. Cells with PU.1-GFP time traces shown in (F) are marked with correspondingly colored arrowheads. Scale bar, 20 μm. (**D**) Heat map showing PU.1-GFP levels over time for all imaged cells. Rectangles define progenitor, macrophage, and B cell populations. (**E**) Alternative hypotheses for PU.1-GFP up-regulation in macrophages. The PU.1 synthesis rate for a single cell is given by $\Delta p/\Delta t$ over the entire observed cell cycle. (**F**) Representative single-cell PU.1-GFP time traces for different cell populations. Data are taken from lineages shown in fig. S9. Horizontal lines give PU.1-GFP level thresholds for the defined cell populations. a.u., arbitrary units. (**G**) Histogram (top) showing distribution of PU.1 synthesis rates in progenitors. Scatter plot showing the relation between PU.1 synthesis rates in mother versus daughter cells. Horizontal and vertical lines indicate the threshold for progenitor subpopulations with higher and lower rates of PU.1 synthesis. (**H**) Plots comparing mean PU.1-GFP levels (top), PU.1 synthesis rates (middle), and cell cycle lengths (bottom) in different cell populations. Red crosses indicate box-plot outliers. Bottom error bars represent 95% confidence intervals. Asterisks indicate significantly different means ($P < 10^{-7}$, one-tailed t test). Data are representative of three independent experiments. N, number of cells.

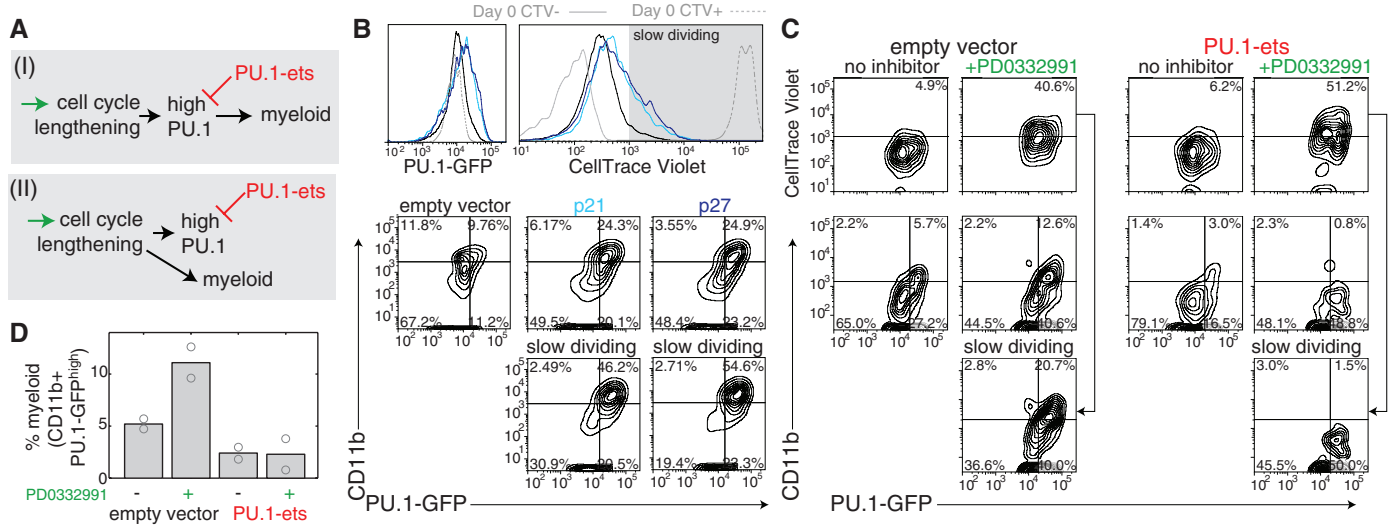

Fig. 2. PU.1 accumulation due to cell cycle lengthening is important for myeloid differentiation. (**A**) Two hypotheses for the function of high PU.1 levels in differentiating macrophages. (**B**) FLPs were transduced with EV, p21, or p27; cultured for 4 days; and analyzed by flow cytometry. Histograms (top) show CellTrace Violet (CTV) (Invitrogen, Carlsbad, California) and PU.1-GFP levels for different transduced populations. The gray shaded area indicates a slow-dividing cell gate. Flow plots (bottom) show CD11b versus PU.1-GFP levels for different transduced cell populations. Percentages of cells in each quadrant are shown. (**C**) FLPs transduced with EV or PU.1 antagonist (PU.1-ets) were cultured for 3 days with or without 2.1 μM CDK4/6 inhibitor PD0332991 and analyzed by flow cytometry. Flow plots show CellTrace Violet (top) or CD11b (bottom) versus PU.1-GFP for the different conditions. (**D**) Effects of PD0332991 and PU.1-ets transduction on the percentage of myeloid cells. Bars represent means of two independent experiments, and circles give individual measurements.

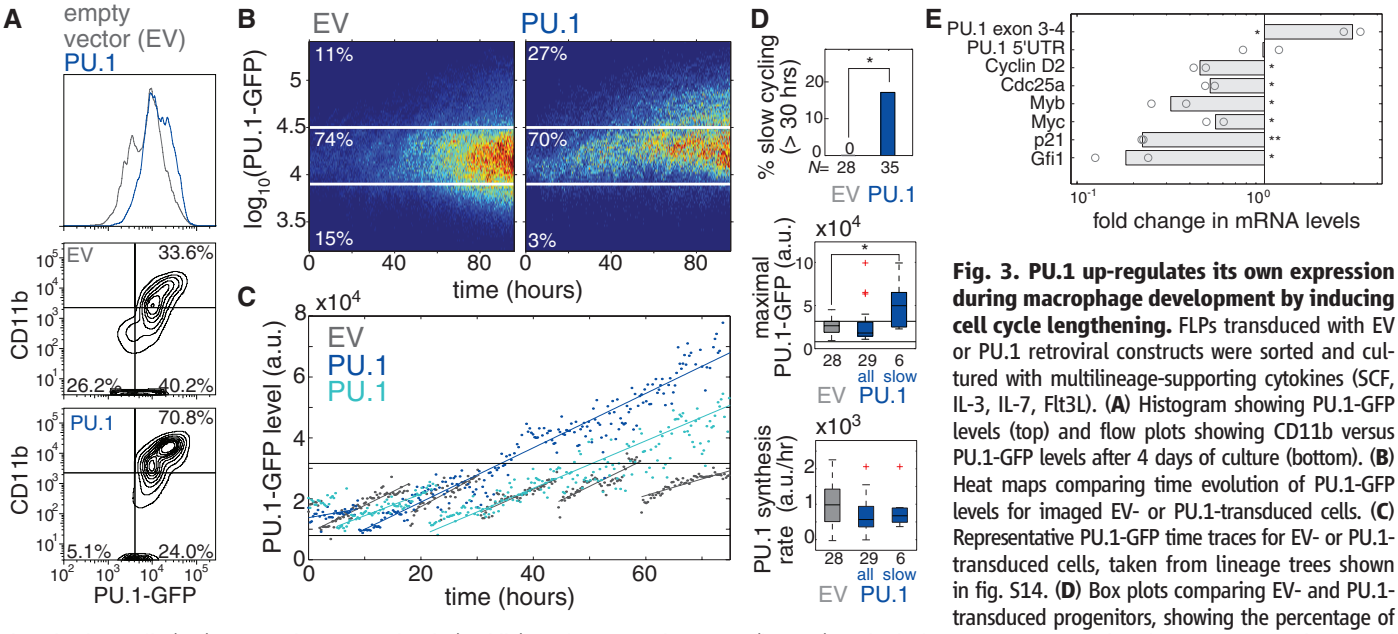

Fig. 3. PU.1 up-regulates its own expression during macrophage development by inducing cell cycle lengthening. FLPs transduced with EV or PU.1 retroviral constructs were sorted and cultured with multilineage-supporting cytokines (SCF, IL-3, IL-7, Flt3L). (**A**) Histogram showing PU.1-GFP levels (top) and flow plots showing CD11b versus PU.1-GFP levels after 4 days of culture (bottom). (**B**) Heat maps comparing time evolution of PU.1-GFP levels for imaged EV- or PU.1-transduced cells. (**C**) Representative PU.1-GFP time traces for EV- or PU.1-transduced cells, taken from lineage trees shown in fig. S14. (**D**) Box plots comparing EV- and PU.1-transduced progenitors, showing the percentage of slow dividing cells (top), maximal PU.1-GFP levels (middle), and PU.1 synthesis rate (bottom) for both the entire PU.1-transduced progenitor population and slow-dividing progenitors alone. Red crosses indicate outliers. Asterisks indicate significantly different means (percent slow dividing, $P < 0.05$, χ^2 test, df = 1; maximal PU.1-GFP, one-tailed t test, $P < 0.005$). Data are representative of two independent experiments. N, number of cells. (**E**) EV- or PU.1-transduced FcγR2/3^{low} FLPs were cultured for 2 days, harvested for RNA, and analyzed with quantitative real-time polymerase chain reaction. Bar chart shows mRNA level fold change for the indicated genes in PU.1-transduced cells compared with EV-transduced cells. Bars represent the means of two independent experiments, and circles represent individual measurements (*$P < 0.1$; **$P < 0.01$; two-tailed t test). UTR, untranslated region.

larger, more rapid protein fluctuations (fig. S17) (*22*). Taken together, these results show how cell cycle–coupled feedback provides a simple mechanism to support multiple stable states that exhibit different rates of cell division.

Besides cell cycle–coupled feedback, cells also contain PU.1 transcriptional feedback, which appears to take effect at lower PU.1 levels (fig. S12). When both feedbacks are incorporated simultaneously, the model can generate three stable steady states with low, medium, and high levels of PU.1 corresponding to the pro-B, progenitor, and macrophage populations, respectively (Fig. 4, B and C). Because of its lower PU.1 threshold, transcriptional feedback allows developing B cells to down-regulate PU.1 while maintaining similar rates of division, consistent with observations. We propose this dual feedback system as a working model for further study of PU.1 regulation during lymphoid and myeloid development.

Could cell cycle–coupled feedback operate in other systems? A similar type of bistability was recently observed in a bacterial synthetic cell cycle–coupled feedback circuit (*29*). In the

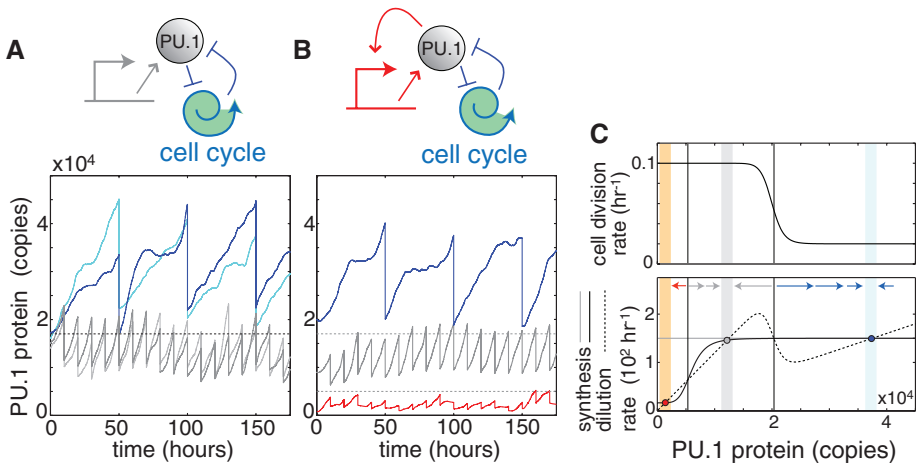

Fig. 4. A cell cycle–coupled feedback loop stably maintains a slow-dividing differentiated state. (**A**) Schematic of a cell cycle–coupled positive-feedback loop (top) and time traces from stochastic simulations of this circuit architecture (bottom), showing four cells with different initial PU.1 levels but identical rate constants. (**B**) Schematic of a hybrid cell cycle–coupled transcriptional positive-feedback circuit (top) and stochastic simulations of this architecture (bottom), showing maintenance of three stable, steady states. (**C**) Phase diagrams for the two circuit architectures, showing PU.1 synthesis rates (black, hybrid; constant thin gray, cell cycle–coupled), as well as dilution rate and cell-division rate (same for both models) against PU.1 levels. Red, gray, and blue circles denote B cell, progenitor, and macrophage steady states, respectively. Arrows indicate the flow of the system. A thorough analysis and discussion of all models is given in the supplementary mathematical appendix (*22*).

context of cell differentiation, other fate regulators have also been shown to promote cell cycle arrest (*30*). Although some transcription factors are notoriously short-lived (e.g., Fos), recent studies have found that many mammalian proteins are stable over multiple cell cycles (*23*, *24*), and other regulatory proteins may resemble PU.1 in this respect. Moreover, induced cell cycle lengthening is known to promote differentiation in other systems (*31*, *32*), suggesting that mechanisms based on accumulation of stable fate regulators during cell cycle arrest may be more prevalent. Where cell fate decisions depend on the balance between two factors with different stabilities, such as PU.1 and the unstable C/EBPα (*33*, *34*), cell cycle speed may act as a tiebreaker, with cell cycle slowdown favoring the more stable factor and acceleration favoring the less stable one. In general, our results imply a mutual regulatory relationship between the cell cycle and transcription factor activities in cell differentiation, and similar relationships may affect other processes that involve cell cycle length changes, such as cancer.

References and Notes

1. H. Singh, R. P. DeKoter, J. C. Walsh, *Cold Spring Harb. Symp. Quant. Biol.* **64**, 13–20 (1999).
2. S. L. Nutt, D. Metcalf, A. D'Amico, M. Polli, L. Wu, *J. Exp. Med.* **201**, 221–231 (2005).
3. J. Back, D. Allman, S. Chan, P. Kastner, *Exp. Hematol.* **33**, 395–402 (2005).
4. Y. Arinobu *et al.*, *Cell Stem Cell* **1**, 416–427 (2007).
5. R. P. DeKoter, H. Singh, *Science* **288**, 1439–1441 (2000).
6. M. K. Anderson, A. H. Weiss, G. Hernandez-Hoyos, C. J. Dionne, E. V. Rothenberg, *Immunity* **16**, 285–296 (2002).
7. C. J. Spooner, J. X. Cheng, E. Pujadas, P. Laslo, H. Singh, *Immunity* **31**, 576–586 (2009).
8. S. Carotta *et al.*, *Immunity* **32**, 628–641 (2010).
9. F. Rosenbauer, D. G. Tenen, *Nat. Rev. Immunol.* **7**, 105–117 (2007).
10. Y. Okuno *et al.*, *Mol. Cell. Biol.* **25**, 2832–2845 (2005).
11. M. A. Zarnegar, J. Chen, E. V. Rothenberg, *Mol. Cell. Biol.* **30**, 4922–4939 (2010).
12. M. Leddin *et al.*, *Blood* **117**, 2827–2838 (2011).
13. P. B. Staber *et al.*, *Mol. Cell* **49**, 934–946 (2013).
14. A. B. Cantor, S. H. Orkin, *Oncogene* **21**, 3368–3376 (2002).
15. K. S. Choe, O. Ujhelly, S. N. Wontakal, A. I. Skoultchi, *J. Biol. Chem.* **285**, 3044–3052 (2010).
16. W. D. Cook *et al.*, *Blood* **104**, 3437–3444 (2004).
17. F. Rosenbauer *et al.*, *Nat. Genet.* **36**, 624–630 (2004).
18. M. J. Walter *et al.*, *Proc. Natl. Acad. Sci. U.S.A.* **102**, 12513–12518 (2005).
19. D. Metcalf *et al.*, *Proc. Natl. Acad. Sci. U.S.A.* **103**, 1486–1491 (2006).
20. M. D. Delgado *et al.*, *Biochem. Biophys. Res. Commun.* **252**, 383–391 (1998).
21. R. P. DeKoter, J. C. Walsh, H. Singh, *EMBO J.* **17**, 4456–4468 (1998).
22. Materials and methods are available as supplementary materials on *Science* Online.
23. E. Eden *et al.*, *Science* **331**, 764–768 (2011).
24. B. Schwanhäusser *et al.*, *Nature* **473**, 337–342 (2011).
25. P. L. Toogood *et al.*, *J. Med. Chem.* **48**, 2388–2406 (2005).
26. F. Kihara-Negishi *et al.*, *Int. J. Cancer* **76**, 523–530 (1998).
27. T. Bellon, D. Perrotti, B. Calabretta, *Blood* **90**, 1828–1839 (1997).
28. C. B. Franco *et al.*, *Proc. Natl. Acad. Sci. U.S.A.* **103**, 11993–11998 (2006).
29. C. Tan, P. Marguet, L. You, *Nat. Chem. Biol.* **5**, 842–848 (2009).
30. L. A. Buttitta, B. A. Edgar, *Curr. Opin. Cell Biol.* **19**, 697–704 (2007).
31. R. A. Steinman, *Oncogene* **21**, 3403–3413 (2002).
32. P. Salomoni, F. Calegari, *Trends Cell Biol.* **20**, 233–243 (2010).
33. R. Dahl *et al.*, *Nat. Immunol.* **4**, 1029–1036 (2003).
34. A. K. Trivedi *et al.*, *Oncogene* **26**, 1789–1801 (2007).

Acknowledgments: We thank R. Butler and S. Washburn for mouse care and J. Verceles, J. Grimm, and D. Perez of the Caltech Flow Cytometry Facility for cell sorting. We also thank members of the Rothenberg and Elowitz labs and L. Goentoro for insightful discussions. The data presented in this manuscript are tabulated in the main paper and the supplementary materials. This work was supported by a Cancer Research Institute/Irvington Postdoctoral Fellowship to H.Y.K.; an Australian Research Council Future Fellowship and the Victorian State Government Operational Infrastructure Support, National Health and Medical Research Council of Australia Independent Research Institute Infrastructure Scheme to S.L.N.; NIH grants to E.V.R. (RC2 CA148278, R33 HL089123, R01 AI083514, and R01 CA90233); the Albert Billings Ruddock Professorship; the Al Sherman Foundation; and the Louis A. Garfinkle Memorial Laboratory Fund.

Supplementary Materials

www.sciencemag.org/cgi/content/full/science.1240831/DC1
Materials and Methods
Mathematical Appendix
Figs. S1 to S18
Tables S1 to S6
References (*35*–*46*)

21 May 2013; accepted 5 July 2013
Published online 18 July 2013;
10.1126/science.1240831

T Follicular Helper Cell Dynamics in Germinal Centers

Ziv Shulman,[1] Alexander D. Gitlin,[1] Sasha Targ,[2] Mila Jankovic,[1] Giulia Pasqual,[2] Michel C. Nussenzweig,[1,3]*† Gabriel D. Victora[2]*†

T follicular helper (T_{FH}) cells are a specialized subset of effector T cells that provide help to and thereby select high-affinity B cells in germinal centers (GCs). To examine the dynamic behavior of T_{FH} cells in GCs in mice, we used two-photon microscopy in combination with a photoactivatable fluorescent reporter. Unlike GC B cells, which are clonally restricted, T_{FH} cells distributed among all GCs in lymph nodes and continually emigrated into the follicle and neighboring GCs. Moreover, newly activated T_{FH} cells invaded preexisting GCs, where they contributed to B cell selection and plasmablast differentiation. Our data suggest that the dynamic exchange of T_{FH} cells between GCs ensures maximal diversification of T cell help and that their ability to enter ongoing GCs accommodates antigenic variation during the immune response.

T cells play a pivotal role in affinity maturation by selecting B cells to enter the germinal center (GC), regulating GC positive selection, and directing B cell differentiation to plasma cells and memory B cells (*1*–*6*). These events are orchestrated by a specialized population

Positive Feedback Between PU.1 and the Cell Cycle Controls Myeloid Differentiation

Hao Yuan Kueh, Ameya Champhekar, Stephen L. Nutt, Michael B. Elowitz and Ellen V. Rothenberg (July 18, 2013)

Science **341** (6146), 670-673. [doi: 10.1126/science.1240831] originally published online July 18, 2013

Editor's Summary

A Different Cycle for Differentiation

The regulated expression of transcription factors determines cell fate decisions during cell differentiation. The transcription factor PU.1 is an important determinant in the differentiation of hematopoietic progenitors to lymphocytes or myeloid cells, where high expression induces macrophage differentiation, whereas low expression leads to the development of B lymphocytes. How PU.1 expression levels are regulated during this cell fate choice, however, is not well understood. **Kueh *et al.*** (p. 670, published online 18 July) found that in mice, reduced transcription of PU.1 led to its reduced expression in developing B lymphocytes, whereas in macrophages, PU.1 was able to accumulate stably because of a lengthening of the cell cycle. Exogenous expression of PU.1 in progenitors supported cell cycle lengthening and macrophage differentiation, and mathematical modeling suggested that such a feedback loop could maintain a slow-dividing macrophage developmental state.